Simultaneous UV–vis Absorption and Raman Spectroelectrochemistry

David Ibañez,[‡] Jesus Garoz-Ruiz,[‡] Aranzazu Heras,* and Alvaro Colina*

Department of Chemistry, Universidad de Burgos, Pza. Misael Bañuelos s/n, E-09001 Burgos, Spain

ABSTRACT: The development of a new device based on the use of UV−vis bare optical fibers in long optical path length configuration and the measurement of the Raman response in normal arrangement allows us to perform UV−vis and Raman spectroelectrochemistry simultaneously in a single experiment. To the best of our knowledge, this is the first time that a spectroelectrochemistry device is able to record both spectroscopic responses at the same time, which further expands the versatility of spectroelectrochemistry techniques and enables us to obtain much more high-quality information in a single experiment. Three different electrochemical systems, such as ferrocyanide, dopamine, and 3,4-ethylenedioxythiophene, have been studied to validate the cell and to demonstrate the performance of the device. Processes that take place in solution can be properly distinguished from processes that occur on the electrode surface during the electrochemical experiment, providing a whole picture of the reactions taking place at the electrode/solution interface. Therefore, this device allows us to study a larger number of complex electrochemical processes from different points of view taking into account not only the UV−vis spectral changes in the solution adjacent to the electrode but also the Raman signal at any location. Furthermore, complementary information, which could not be unambiguously extracted without considering together the two spectroscopic signals and the electrochemical response, is obtained in a novel way.

A single spectroelectrochemistry experiment contains electrochemical and spectroscopic information about a chemical system, allowing the study of a wide range of processes from, at least, two different points of view.[1,2] As can be inferred, versatility is truly huge because multiple electrochemical techniques can be used, as well as different spectral regions can be analyzed depending on the system under study and the desired information to be obtained.[3,4]

UV−vis absorption spectroelectrochemistry has been used throughout history to study a great variety of chemical systems in a wide variety of research fields such as, for example, reaction mechanisms, diffusive and adsorptive processes, substances of biological interest, characterization of compounds, optical and electrical properties of materials, and evaluation of parameters of electron-transfer reactions.[3] Several applications related to quantitative analysis using spectroelectrochemistry have emerged in recent years, probably due to the autovalidated results obtained with UV−vis spectroelectrochemistry and the use of powerful multivariate statistical tools for the data analysis.[5−7] Normal and parallel configurations are the main spectroelectrochemistry arrangements, while the simultaneous combination of both is called bidimensional spectroelectrochemistry.[8,9] As is well known, normal configuration includes information related to the spectral changes occurring in the solution and at the electrode since the light beam samples the system perpendicularly to the electrode surface. In parallel configuration, only the spectral changes occurring in the solution are recorded because now the light beam only samples the first micrometers of the closest solution layer to the electrode surface.

Raman spectroelectrochemistry is a powerful technique that allows us not only to characterize steady-state systems but also to perform in situ studies of different evolving processes. The dynamic character of time-resolved Raman spectroelectrochemistry provides a large number of full spectra that enables us to describe the spectroscopic evolution of a chemical system with time or potential together with the electrochemical signal.[10−14] The versatility achieved by Raman spectroelectrochemistry through the development of new devices has allowed researchers to study systems of different nature.[14−21] Moreover, the information provided by Raman spectroelectrochemistry is fully complementary to the one obtained using UV−vis spectroelectrochemistry.

Undoubtedly, the relevant advantages of UV−vis absorption and Raman spectroelectrochemistry have been widely exploited separately to date. In fact, several devices have been fabricated with the aim of performing UV−vis or Raman spectroelectrochemistry experiments, being even possible to use the same cell for both spectroelectrochemistry disciplines,[22–25] but always separately. To the best of our knowledge, as of today there are no devices capable of carrying out UV−vis and Raman spectroelectrochemistry simultaneously. However, taking into account the advantages of obtaining all data simultaneously, we can affirm that the development of a UV−vis/Raman spectroelectrochemistry device able to perform this type of experiments is of great interest to shed more light on complex reaction mechanisms.

Accordingly, the novel spectroelectrochemistry cell and the work presented in this paper enable us to obtain complementary electrochemical and spectroscopic responses by collecting simultaneously time-resolved UV−vis and Raman spectra during an electrochemical experiment. On the one hand, a UV−vis light beam, sent and collected by bare optical fibers, only samples the first micrometers of the solution adjacent to the electrode surface in parallel configuration. On the other hand, Raman spectra in normal arrangement contain vibrational information about the desired area. As can be inferred, the large amount of data obtained helps to distinguish the processes that take place in solution from those occurring on the electrode surface by analyzing the spectral changes of different nature (absorption and dispersion) obtained during a single experiment.

In this work, a glassy carbon foil or a single-walled carbon nanotube (SWCNT) film have been used as working electrodes. The use of carbon materials in electrochemistry has numerous advantages.[26] Carbon nanotubes are structures with an array of fascinating mechanical, electrical, electronic, and thermal properties that make them an outstanding material for electrochemical purposes.[27–35] In fact, our group has developed different methodologies to fabricate SWCNT electrodes by transferring SWCNT films obtained by filtration on different supports.[6,9,36,37] These SWCNT films can also be modified with other carbon nanomaterials.[38]

We have selected three electrochemical systems to illustrate, in a general way, some of the problems that researchers would be able to investigate using the combination of UV−vis and Raman spectroelectrochemistry. The electrochemical systems have also been useful to determine the suitable performance of the new UV−vis/Raman spectroelectrochemistry device. Therefore, a typical redox couple used for the validation of spectroelectrochemical devices (ferricyanide/ferrocyanide), the oxidation of a biomolecule such as dopamine on a SWCNT electrode, and a complex electrochemical reaction as, for instance, the electropolymerization of 3,4-ethylenedioxythiophene (EDOT) have been studied using simultaneously UV−vis and Raman spectroelectrochemistry.

Ferricyanide/ferrocyanide redox couple is a one-electron and well-defined electrochemical system often used as a probe in aqueous solution.[39] This first electrochemical system has been used to study a process that occurs only in solution. Meanwhile, dopamine is a neurotransmitter involved in regulating behavior, movement, and immune functions, among others.[40] Abnormal dopamine levels are associated with diseases with high prevalence in the world today, such as schizophrenia[41] and Parkinson's disease.[42,43] Finally, poly(3,4-ethylenedioxythiophene) (PEDOT) is one of the most used conducting polymers due to its exceptional properties. It shows high conductivity, electrochemical stability, high transparency, catalytic ability, and good electrochromic properties.[44–46] Indeed, PEDOT is transparent in its doped state and colored in its neutral state, and it is characterized by a relative low band-gap value.[47] The oxidation of dopamine on a SWCNT electrode and the electropolymerization of EDOT have been used to study the different processes that take place in solution and on the electrode surface.

The main objective of this work is to demonstrate the correct performance of the new UV−vis/Raman spectroelectrochemistry device, showing the capabilities and advantages of this novel technique.

EXPERIMENTAL SECTION

Reagents and Materials. SWCNTs (Sigma-Aldrich), 1,2-dichloroethane (DCE, 99.8% for HPLC, Acros Organics), nitrocellulose membrane (filter pore size 0.8 μm, Millipore), quartz plate (Sugelabor), silver conductive paint (Electrolube), and transparent nail polish (Procesos Cosméticos) were used to fabricate the SWCNT working electrode (WE). Apart from this electrode, a glassy carbon foil (Goodfellow) properly polished to a mirror finish using alumina slurries with different powder size down to 0.5 μm was also used as WE. Potassium ferrocyanide (Merck), LiCl (Merck), dopamine (99%, Acros Organics), $HClO_4$ (60%, Panreac), EDOT (99%, Acros Organics), and $LiClO_4$ (Panreac) were used to prepare the solutions. Poly(methyl methacrylate) (PMMA) plates, polytetrafluoroethylene (PTFE, Teflon) plates, O-rings, nuts, and bolts were used to fabricate the cell developed in this work, which was fabricated using a CO_2 laser cutting machine.

All reagents were used as received. All chemicals were of analytical grade. Aqueous solutions were freshly prepared, or stored at 4 ºC, using ultrapure water (18.2 MΩ cm resistivity at 25 °C, Milli-Q Direct 8, Millipore).

Instrumentation. All spectroelectrochemistry experiments were performed at room temperature. Spectroelectrochemistry setup includes a potentiostat/galvanostat (PGSTAT20, Metrohm Autolab) coupled to the equipment to record the spectral changes. On the one hand, UV−vis absorption spectra were obtained using a deuterium light source (AvaLight-DH-S-BAL, Avantes), bare optical fibers (100 μm in diameter, Ocean Optics), and a spectrometer (QE65000 198−1006 nm, Ocean Optics). On the other hand, dynamic Raman spectra were obtained using a Confocal Raman Voyage (BWTEK). A laser source emitting at the wavelength of 532 nm with a power of 15 mW was employed to obtain the spectra, using a 20X objective. The spectral resolution was 3.8 cm^{-1}. An XYZ piezoelectric positioner (Newport 271) controlled by a Newport motion controller (Newport, ESP 301) was used to focus the laser beam with micrometric resolution. Further details about the dynamic spectroelectrochemical Raman system have been previously reported.[10,11] A tip-sonicator (CY-500, Optic ivymen System) was used to properly disperse the SWCNTs.

Safety Considerations. All handling and processing were performed carefully, particularly when DCE was used.

Electrodes Preparation. Two different WEs are used in this work. The first one, a glassy carbon foil, was properly polished with alumina, thoroughly rinsed with ultrapure water, and dried. SWCNT electrodes are the second type of electrodes used. Briefly, the methodology employed to fabricate these SWCNT electrodes[9] involves the filtration under vacuum of 0.8 mL of a sonicated SWCNT homogeneous dispersion in DCE (5 mg/L) through a nitrocellulose filter. The homogeneous SWCNT film, whose transparency and conductivity depend on the filtered volume of the SWCNT dispersion, was immediately low-pressure transferred on a quartz plate applying only a slight finger pressure. After letting the SWCNT film and the filter dry at room temperature, the filter was carefully separated from the quartz support using tweezers. Therefore, homogeneous, clean, and reproducible SWCNT films of 10 mm in diameter on quartz were obtained in a quick and inexpensive way. The electrical contact was made from the SWCNT film to the edge of the quartz plate with silver conductive paint, which was dried in an oven at 75 ºC for 45 min. Finally, the silver contact was electrically isolated using nail polish, which was dried at room temperature.

Fabrication of the Device for UV−vis/Raman Spectroelectrochemistry Measurements. Figures 1a and 1b show the illustrations of the disassembled and assembled UV−vis/Raman spectroelectrochemistry cell, respectively. The device consists of four main parts. The piece placed at the bottom (1) is the WE support and can be made of PTFE or PMMA. In this case, the material employed is not important because this piece is only used as a support and it is not in contact with the solution. An O-ring (2) helps to fix the WE with the two bare optical fibers between the bottom piece (1) and the next one (3), avoiding solution leakages. One of the optical fibers is connected to the light source, and the other one to the spectrometer. The second piece (3) is made of PTFE. A hole of 6.40 mm in diameter is drilled in its center and a small recess is made for the placement of another O-ring (4), particularly useful for the assembly with the third piece (5) and to prevent a possible leakage of the solution. This third piece (5), also made of PTFE, has a drilled hole of 18.50 mm in diameter to contain the bulk solution and a small recess for the placement of another O-ring (6). Finally, the last piece (7) is an optical window that is placed on top of the cell. Four small holes of 2.20 mm in diameter are drilled in this piece (7) for the placement of the reference (RE) and the counter (CE) electrodes, to facilitate the filling and emptying of the cell (approximate volume of 1.2 mL), and to deoxygenate the solution. Although none of the processes studied in this work required deoxygenated solutions, it can be easily performed using the unoccupied holes to introduce an inert gas that removes the oxygen and to allow the gas flow to leave the device. For the experiments shown in this work, this piece is made of PMMA but, taking into account that some organic solvents dissolve the PMMA, a quartz window can be used in these cases. Pieces 1, 3, 5, and 7 have holes in their corners to allow the whole device to be assembled with nuts and bolts. In all experiments, a homemade Ag/AgCl/KCl 3 M is used as RE and a platinum wire as CE. As previously mentioned, a glassy carbon foil (shown in Figure 1) or a SWCNT film supported on quartz (shown in a previous work)[9] are used as WE. Figure S1 of the Supporting Information displays an expanded diagram of the optical fibers, UV−vis light beam, laser beam, and WE to show how the two beams are interrogating both the solution and the SWCNT WE. In addition, the bottom piece (1) has a drilled hole in its center to place a commercial electrode if necessary. Many different WEs (gold, platinum, etc.) can be used depending on the desired information to be obtained. The versatility is high for commercial and homemade WEs. The main limitation is that WEs have to be flat to allow the parallel light beam to sample the adjacent solution to the electrode. Therefore, a wire or a mesh, for example, are not intended to be used as WEs. The possibility of using different WEs demonstrates the utility and versatility of this new cell to carry out simultaneously UV−vis and Raman spectroelectrochemistry measurements.

It should be noted that the UV−vis spectroelectrochemistry setup is based on bare optical fibers of 100 µm in diameter. The use of bare optical fibers has clear advantages such as, for example, the facility to align the light beams and to change the optical path length, which is defined as the distance between both optical fibers.[6,9,48] Furthermore, absorptometric measurements in parallel configuration offer several advantages with respect to normal configuration: (i) longer optical path length and thus higher sensitivity, allowing the study of compounds with low molar absorption coefficients; (ii) optically transparent electrodes are not required; and (iii) the UV−vis light beam only samples the first 100 µm of the solution adjacent to the WE surface, without interfering with the Raman signal.

Moreover, the most important features of this novel cell related to the Raman spectroelectrochemistry setup can be summarized as: (i) the short distance between the WE surface and the optical window favors the collection of Raman photons; (ii) the flatness required to perform Raman spectroscopy measurements is guaranteed by this optical window (piece 7, Figure 1a); and (iii) the UV−vis light beam provided by the optical fibers does not disturb the Raman signal at all.

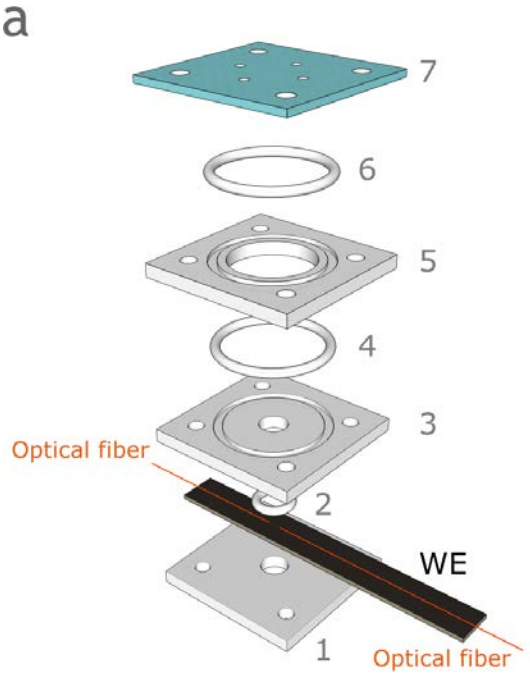

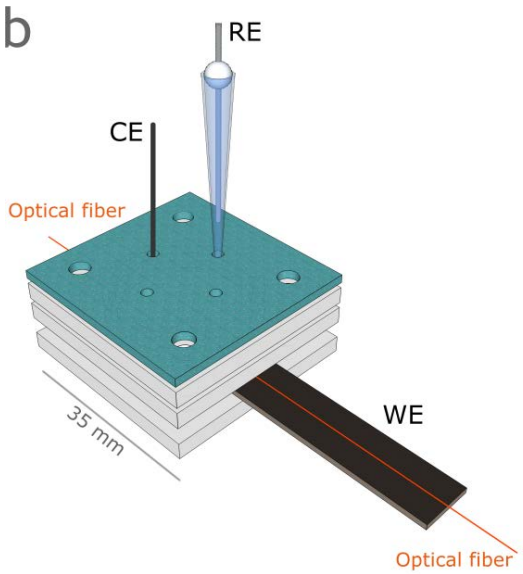

Figure 1. Schematic view of the (a) disassembled and (b) assembled UV−vis/Raman spectroelectrochemistry cell.

Hence, the cell design is optimal to ensure the flatness of the solution needed for Raman measurements, to place the UV−vis bare optical fibers in parallel configuration, to completely disassemble the device to be cleaned, to avoid solution leakages, and to easily deoxygenate the solution. As is shown below, this device enables us to perform UV−vis/Raman spectroelectrochemistry simultaneously, providing relevant information for the study of complex electrochemical processes from different points of view.

RESULTS AND DISCUSSION

Ferricyanide/ferrocyanide redox couple. The ferricyanide/ferrocyanide redox couple is an ionic probe commonly used in spectroelectrochemistry because it is a quasi-reversible system whose two redox forms are spectroscopically distinguishable.[39] For this reason, it was initially used to validate the new cell, allowing us to obtain similar information about the electrochemical process with UV−vis absorption and Raman responses.

Spectroelectrochemistry measurements of 2.5×10^{-2} M potassium ferrocyanide in 0.1 M LiCl were performed using the novel UV−vis/Raman spectroelectrochemistry device with a glassy carbon foil as WE. Figure 2 shows the cyclic voltammogram between −0.20 V and +0.80 V at a potential scan rate of 0.02 V s^{-1} (Figure 2a), and the 3D spectra evolution with time/potential related to the UV−vis spectral region (Figure 2b) and to the Raman signal (Figure 2c). The integration time for UV−vis absorptometric spectra was 500 ms and for Raman spectra was 800 ms. These values indicate the high time-resolved data acquisition offered by this experimental setup. The optical path length was 0.5 mm. The spectrum of the initial solution was taken as reference for the UV−vis absorption spectra, and the spectra evolution of both UV−vis and Raman spectral regions was recorded concomitantly with the electrochemical signal in a single experiment.

Ferrocyanide undergoes the electrochemical process illustrated in the cyclic voltammogram of Figure 2a. The anodic peak is observed at +0.392 V, while the reduction peak occurs at +0.097 V. In addition, on the one hand, two UV−vis absorption bands related to ferricyanide emerge at 310 and 420 nm (Figure 2b). On the other hand, the Raman spectra evolution (Figure 2c) shows the spectral changes in the band centered at 2132 cm^{-1}, related to ferricyanide, as well as in the bands centered at 2056 and 2093 cm^{-1}, associated with ferrocyanide. The corresponding UV−vis cyclic voltabsorptograms at the wavelengths of interest and the evolution of the Raman bands with potential are illustrated, respectively, in Figures S2 and S3 of the Supporting Information.

The oxidation of ferrocyanide to ferricyanide occurs from +0.15 V of the forward scan up to +0.35 V of the backward scan taking into account the three simultaneous responses. The absorbance of the UV−vis bands at 310 and 420 nm, and the Raman intensity of the band at 2132 cm^{-1}, related to ferricyanide species, increase in this potential range in accordance with the oxidation process of ferrocyanide to ferricyanide, which diffuses from the electrode surface to the bulk solution. As expected, the intensity of the Raman bands centered at 2056 and 2093 cm^{-1}, related to ferrocyanide, simultaneously decreases throughout the same time frame. Finally, a decrease of the absorbance at 310 and 420 nm (clearly observed in the corresponding cyclic voltabsorptograms shown in Figure S2 of the Supporting Information), the simultaneous bleaching of the intensity at 2132 cm^{-1}, as well as an increase of the intensity at 2056 and 2093 cm^{-1}, are observed from +0.35 V of the backward scan onwards, due to the consumption of the electrogenerated ferricyanide that is reduced to ferrocyanide.

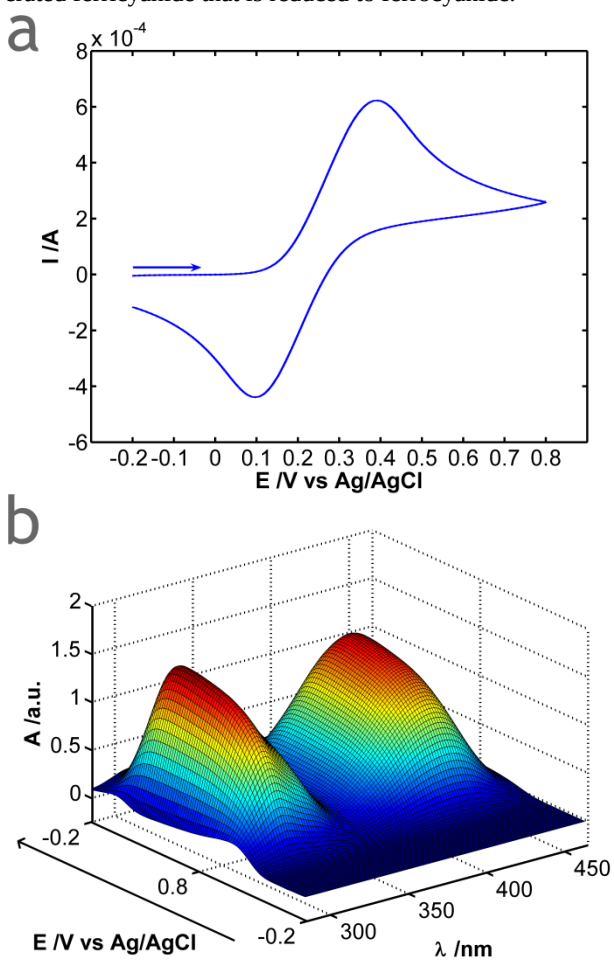

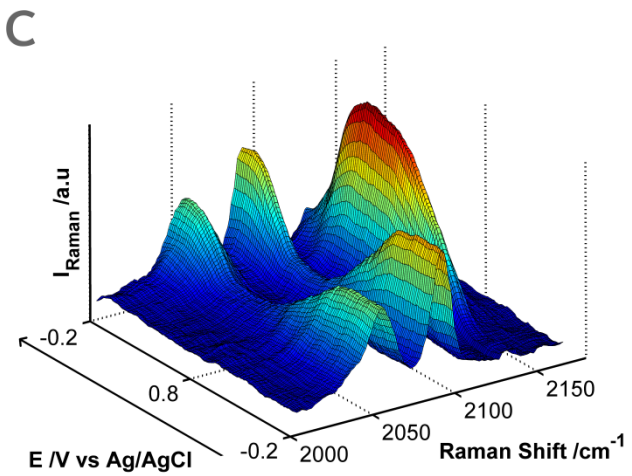

Figure 2. (a) Cyclic voltammogram of 2.5×10^{-2} M potassium ferrocyanide in 0.1 M LiCl between −0.20 V and +0.80 V at 0.02 V s^{-1} on a glassy carbon foil as WE. Three-dimensional spectra evolution with potential of (b) UV−vis absorptometric measurements and of (c) Raman signal during the potentiodynamic experiment.

Therefore, the same conclusions can be extracted from the UV−vis and Raman responses about the electrochemical process of the ferricyanide/ferrocyanide redox couple during this spectroelectrochemistry experiment. To sum up, the suitable performance of this UV−vis/Raman spectroelectrochemistry device has been properly validated taking into account the results obtained in this experiment.

Oxidation of dopamine on a SWCNT electrode. UV−vis/Raman spectroelectrochemistry was used to study the electrochemical reaction of dopamine on a SWCNT electrode. In this case, different and complementary information was obtained with both spectroscopic responses. The integration times were 150 and 1440 ms for UV−vis and Raman signals, respectively, and the optical path length in UV−vis measurements was set to 0.4 mm.

Spectroelectrochemistry measurements were carried out using a SWCNT WE prepared on quartz. Figure 3a shows the cyclic voltammogram of 6.6×10^{-4} M dopamine in 1 M $HClO_4$ between +0.10 V and +1.00 V at 0.01 V s^{-1}. UV−vis and Raman spectra obtained during the oxidation scan are plotted in Figures 3b and 3c, respectively. The corresponding spectra evolution during the reduction scan can be found in Figures S4 and S5 of the Supporting Information. As in the previous experiment, the spectrum of the initial solution was taken as reference for the UV−vis absorption spectra.

The electrochemical reaction of dopamine is a well-known process that can generate different products depending on the pH value. The cyclic voltammogram, Figure 3a, displays one oxidation peak, which involves a two-electron transfer, related to the generation of dopaminequinone as a single product, as was expected under these experimental acidic conditions.[49] The peak potential difference takes a value of 0.303 V, indicating a quasi-reversible electrochemical behavior.

The UV−vis spectra evolution recorded during the oxidation scan show, in accordance with the electrochemical signal, the evolution of three bands at 248, 283, and 391 nm from +0.50 V onwards (Figure 3b). UV−vis bands at 248 and 391 nm are related to the electrogeneration of dopaminequinone, and the one at 283 nm is associated with the consumption of dopamine.[5,50] As can be seen in Figure S4 of the Supporting Information, the spectral changes evolve in the opposite way during the cathodic scan due to the reduction of the electrogenerated dopaminequinone and regeneration of dopamine. It should be noted that an excellent spectral resolution is achieved, not only in the visible but also in the ultraviolet spectral region.

Moreover, a maximum and constant value of absorbance is reached due to the steady-state achieved when dopaminequinone diffuses beyond the first 100 μm of the solution closest to the SWCNT electrode surface sampled by the optical fibers. A first approximation of the molar absorption coefficient value of dopaminequinone can be calculated using the Beer−Lambert law (A=εlC) and assuming that a dopamine concentration of 6.6×10^{-4} M is converted to dopaminequinone in the 100 μm of the solution adjacent to the electrode surface sampled by the optical fibers. From the maximum and constant value of absorbance at 391 nm (0.0275 au), the concentration of dopamine (6.6×10^{-4} M), and the optical path length in parallel configuration (0.04 cm), an experimental value of roughly 1040 M^{-1} cm^{-1} is estimated for the molar absorption coefficient of dopaminequinone at 391 nm.

In order to obtain Raman information about this system, the laser was focused on the SWCNT electrode surface, but there is no Raman signal related to dopamine at this low concentration. Nevertheless, Raman spectra provide essential information about the behavior of SWCNTs with potential during the experiment (Figure 3c and Figure S5 of the Supporting Information). The behavior of the SWCNTs during the electron transfer is not easily obtained using other analytical

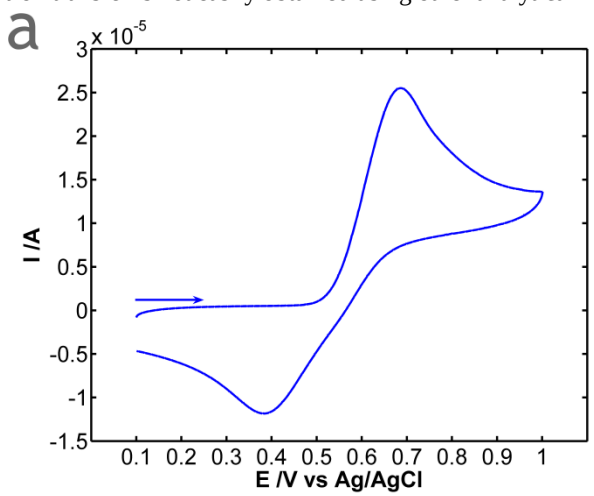

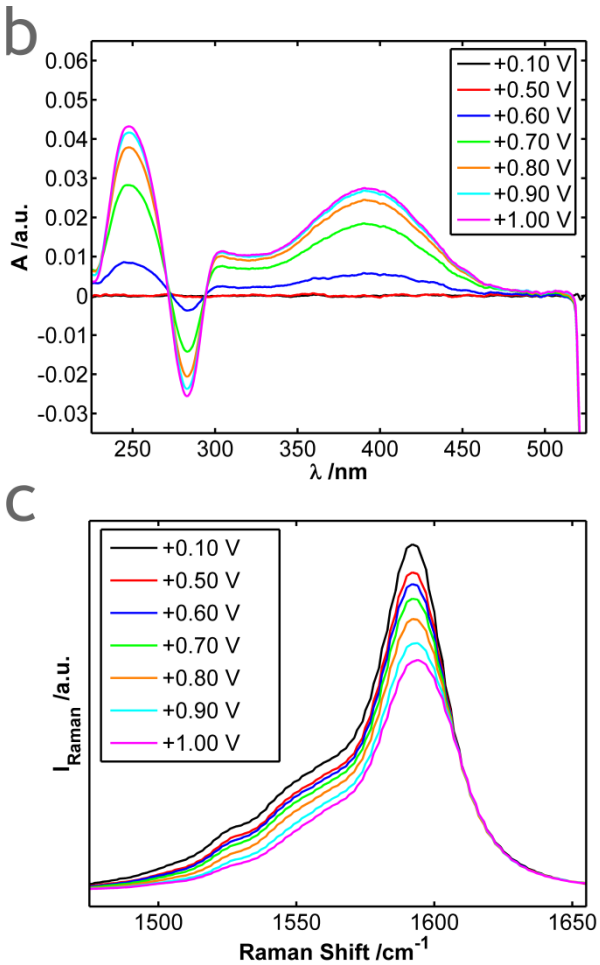

Figure 3. (a) Cyclic voltammogram of 6.6×10^{-4} M dopamine in 1 M $HClO_4$ between +0.10 V and +1.00 V at 0.01 V s^{-1} on a SWCNT WE prepared on quartz. (b) UV−vis and (c) Raman spectra evolution recorded during the oxidation scan.

techniques. Raman spectrum of SWCNTs (Figure S6 of the Supporting Information) shows four main bands:[51,52] the radial breathing mode (RBM) at 150−300 cm^{-1}; the disorder induced mode (D) at 1300−1400 cm^{-1}; the tangential displacement mode (G) at 1550−1600 cm^{-1}; and the high-frequency two-phonon mode (G' or 2D) at 2550−2750 cm^{-1}. In order to illustrate the behavior of SWCNTs during the electrochemical oxidation of dopamine, the most intense band (G-band) was analyzed (Figure 3c). Oxidation (p-doping) of SWCNTs leads to a decrease of the G-band Raman intensity. During the cathodic scan, the G-band intensity returns to approximately the initial value (Figure S5 of the Supporting Information). All these changes in the Raman intensity are only related to the electrochemical doping/de-doping of the SWCNT WE.[11,51]

In addition, only the generation of dopaminequinone is allowed under these acidic conditions, avoiding the formation of dopaminechrome that could polymerize on the SWCNT WE. The absence of the dopaminechrome absorption around 470 nm in the UV−vis spectra[5] and of the characteristic bands in Raman spectroscopy when dopaminechrome polymerizes on the electrode confirms, with two independent techniques in the same experiment, that the oxidation of dopamine under acidic conditions only generates dopaminequinone.

In summary, this spectroelectrochemistry experiment allows us to obtain different information depending on the spectroscopic technique used. Information extracted from UV−vis spectral evolution is mainly related to spectroscopic changes that take place in the solution adjacent to the electrode, which are associated with compounds present in the solution (dopamine and products derived from its electrochemical reaction). Moreover, the evolution of the Raman spectra is related to the oxidation state of the SWCNT WE surface. Therefore, we can conclude that we are able to observe two different processes in a single electrochemical experiment taking into account both spectroscopic signals. This is a great advantage of this device because the parallel UV−vis light beam does not sample the SWCNT surface and Raman spectroscopy is not capable of following the electrochemical reaction of dopamine. Nevertheless, as has been demonstrated, this experimental device allows us to study both processes simultaneously without interference between the two optical techniques.

Electropolymerization of EDOT in aqueous solution. This experiment was performed to observe an electrochemical process from two different but correlated spectroscopic points of view. PEDOT, the electrogenerated conducting polymer, is widely used for many applications[53–57] and it has been previously studied by spectroelectrochemistry.[47]

Cyclic voltammetry of 3×10^{-3} M EDOT in 0.2 M $LiClO_4$ was performed at a scan rate of 0.025 V s^{-1} on a SWCNT WE prepared on quartz, using the following potentials: initial and final potential ($E_i = E_f = 0.00$ V); anodic vertex potential ($E_{v1} = +1.00$ V); and cathodic vertex potential ($E_{v2} = -0.50$ V). UV−vis and Raman spectra were recorded every 300 and 1920 ms, respectively. The optical path length in UV−vis measurements was 1.1 mm. As in the previous cases, the spectrum of the initial solution was taken as reference for the UV−vis absorption spectra.

The cyclic voltammogram is plotted in Figure 4a. An increase in the anodic current is observed from ca. +0.70 V onwards, according to the oxidation process of EDOT. The UV−vis cyclic voltabsorptogram at 254 nm (main band of the UV−vis spectrum of EDOT),[58,59] Figure 4b, and the evolution of the Raman bands centered at 1110 and 1134 cm^{-1} with potential, Figure 4c, show optical changes that are correlated with the electrochemical response.

The evolution of the UV band at 254 nm (Figure 4b), indicates that the consumption of the monomer takes place from +0.85 V onwards, concomitantly with the oxidation process appreciated in the electrical signal (Figure 4a). Thus, in the potential window between +0.85 V and +1.00 V in the anodic and cathodic scan, absorbance at 254 nm decreases because of the consumption of EDOT in the solution closest to the WE surface. Once absorbance at 254 nm reaches a minimum value, its evolution is only related to the diffusion of EDOT from the bulk solution to the electrode-solution interface.

As can be observed in Figure 4c, Raman signal provides complementary information about this process. The evolution of the Raman spectra was also recorded simultaneously with the cyclic voltammetry. Figure S7a and Table S1 of the Supporting Information display, respectively, the Raman spectra and the vibrational assignment of the main bands corresponding to neutral (−0.50 V) and doped (+1.00 V) PEDOT.[60] In the Raman spectra registered (Figure S7a), it can also be observed

the characteristic bands of SWCNTs, some of them overlapped with those of PEDOT. Although more intense bands are observed in the Raman spectra, Figure S7b of the Supporting Information displays the contour plot of only the Raman signal in a Raman shift frame where less interference of SWCNTs is appreciated. Here it can be observed the evolution of the 1110 and 1134 cm^{-1} bands with time. These two Raman bands were studied, specifically because the 1110 cm^{-1} band is related to the neutral PEDOT and the 1134 cm^{-1} band is associated with the doped PEDOT (Figure 4c). Analyzing the Raman band at 1110 cm^{-1} with potential (Figure 4c), we can observe that initially, from 0.00 V to +0.70 V, this band is not detected. This band is clearly observed when electropolymerization have occurred and the electrogenerated polymer is being neutralized. This process of PEDOT de-doping lasts up to the second vertex potential, −0.50 V. Next, Raman intensity decreases indicating that PEDOT is starting to be doped again. The evolution of the band centered at 1134 cm^{-1} is more sensitive to the doped polymer and it shows a clearly different behavior. The intensity of this Raman band increases from ca. +0.65 V onwards because of the doping of PEDOT. Next, the intensity of the 1134 cm^{-1} band decreases when the neutral form begins to be generated.

The charge involved in the polymerization process can be extracted from the cyclic voltammogram (Figure 4a). However, the electrochemical signal does not provide a well-defined response to determine the potentials at which the polymerization takes places. Evolution of the Raman intensity (Figure 4c) allows us to define the potentials when the doped PEDOT is electrogenerated, and, in this way, to calculate the charge involved in this electrochemical process. According to the evolution of the 1134 cm^{-1} band in the Figure 4c, the polymerization occurs from ca. +0.65 V (anodic scan) to +0.90 V (cathodic scan). The charge involved in the polymerization is calculated from the cyclic voltammogram, obtaining 5.1×10^{-4} C as the experimental value of the charge involved in the EDOT oxidation during the polymerization.

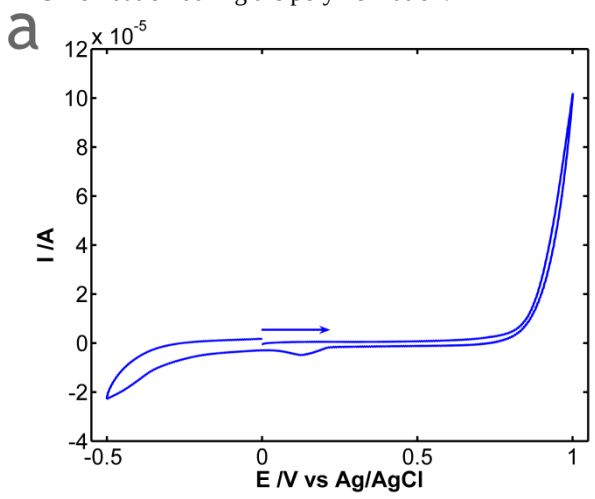

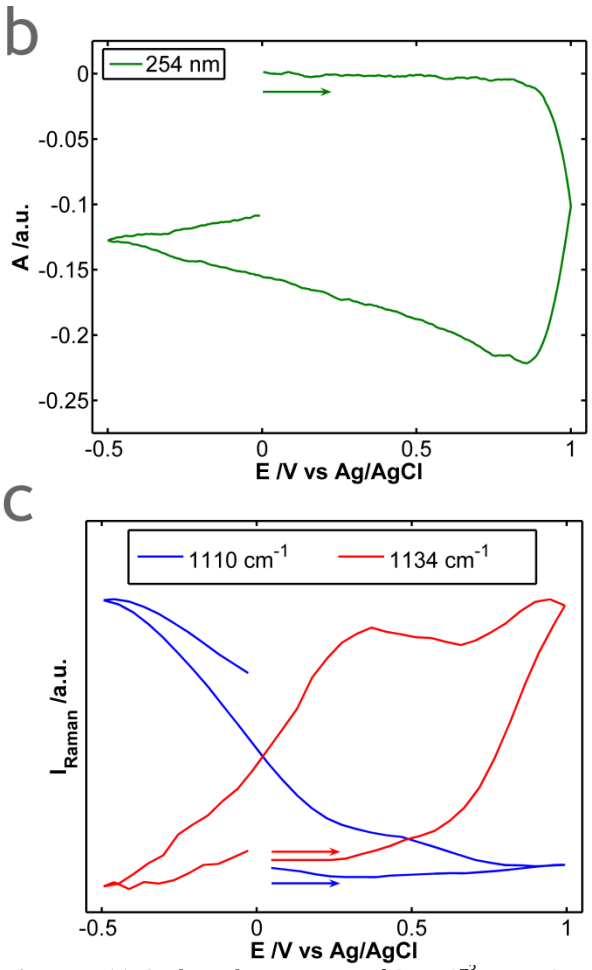

Figure 4. (a) Cyclic voltammogram of 3×10^{-3} M EDOT in 0.2 M $LiClO_4$ ($E_i = E_f = 0.00$ V, $E_{v1} = +1.00$ V, and $E_{v2} = -0.50$ V) at 0.025 V s^{-1} on a SWCNT WE prepared on quartz. (b) UV−vis cyclic voltabsorptogram at 254 nm and (c) evolution of the Raman bands at 1110 and 1134 cm^{-1} recorded during the reaction.

This last experiment allows us to follow the evolution of an electropolymerization process by means of UV−vis and Raman spectroscopic responses, which enables us to observe two different perspectives on the same electrochemical process. Thus, the UV−vis spectra evolution with potential is associated with the consumption of EDOT in the solution layer adjacent to the SWCNT WE. However, the Raman response is related to the generation of PEDOT electrodeposited on the SWCNT WE giving also information about its doping level at each potential. In conclusion, the EDOT electropolymerization process is studied by UV−vis and Raman spectroscopy, obtaining complementary, useful, and valuable information.

CONCLUSIONS AND FUTURE WORK

In this work, UV−vis absorption and Raman dispersion spectroelectrochemistry measurements have been performed simultaneously. A novel and easy-to-use device, based on UV−vis bare optical fibers in long optical path arrangement and on measuring the Raman signal in normal configuration, has been fabricated, allowing to carry out this type of hybrid UV−vis/Raman spectroelectrochemistry experiments. A glassy carbon foil or a SWCNT film transferred on quartz have been

used as WEs, and good results have been achieved with three different electrochemical reactions. Ferrocyanide has been employed to validate the device because the same spectral information about its electrochemical process was obtained with the two spectroscopic techniques. A second experiment has been performed to study the electrochemical reaction of dopamine in acidic media on a SWCNT electrode. In this case, each spectroscopic technique has been used to follow a different process, and therefore completely different information was obtained. The generation of dopaminequinone as the single oxidation product has been observed by the evolution of the UV−vis spectra in the solution layer, while the electrochemical behavior of the SWCNT WE has been followed using the Raman response. Finally, the UV−vis/Raman spectroelectrochemistry device has been used to study the electropolymerization of EDOT in aqueous solution on a SWCNT WE. The EDOT consumption in the first 100 μm of the solution adjacent to the WE was studied by the parallel UV−vis light beam, and the information about the electrogeneration of PEDOT was extracted from the Raman signal.

This UV−vis/Raman spectroelectrochemistry device, which is definitely a significant advance in this research field, greatly increases the multiresponse, in situ, versatile, and real-time character of spectroelectrochemistry. The excellent performance of this device has been clearly demonstrated with the electrochemical, UV−vis, and Raman responses obtained simultaneously in all cases. This spectroelectrochemistry cell could be widely used by the scientific community in the near future to shed more light about complex reactions and their mechanisms, as well as to characterize new materials. Curiously, a question is able to give an idea about the large number of potential applications: Why look for a single signal when you can study three simultaneous and complementary responses in a simple way?

ASSOCIATED CONTENT

Supporting Information

The Supporting Information is available free of charge on the ACS Publications website. Figures and table (PDF)

AUTHOR INFORMATION

Corresponding Authors

*E-mail: maheras@ubu.es
*E-mail: acolina@ubu.es
Tel: +34 947 25 88 17. Fax: +34 947 25 88 31.

Author Contributions

‡David Ibañez and Jesus Garoz-Ruiz contributed equally to this work.
The manuscript was written through contributions of all authors. All authors have given approval to the final version of the manuscript.

Notes

The authors declare no competing financial interest.

ACKNOWLEDGMENTS

Support from Ministerio de Economía y Competitividad (CTQ2014-55583-R, CTQ2014-61914-EXP, CTQ2015-71955-REDT) is gratefully acknowledged. D.I. thanks Ministerio de Economía y Competitividad for his post-doctoral fellowship (CTQ2014-61914-EXP). J.G.-R. thanks Ministerio de Educación, Cultura y Deporte for his pre-doctoral FPU fellowship.

REFERENCES

(1) Kuwana, T.; Darlington, R. K.; Leedy, D. W. *Anal. Chem.* **1964**, *36*, 2023–2025.
(2) Heineman, W. R. *Anal. Chem.* **1978**, *50*, 390A–402A.
(3) Keyes, T. E.; Forster, R. J. In *Handbook of Electrochemistry*; Zoski, C. G., Ed.; Elsevier: Amsterdam, 2007; pp 591–635.
(4) Dunsch, L. *J. Solid State Electrochem.* **2011**, *15*, 1631–1646.
(5) González-Diéguez, N.; Colina, A.; López-Palacios, J.; Heras, A. *Anal. Chem.* **2012**, *84*, 9146–9153.
(6) Garoz-Ruiz, J.; Izquierdo, D.; Colina, A.; Palmero, S.; Heras, A. *Anal. Bioanal. Chem.* **2013**, *405*, 3593–3602.
(7) Asadpour-Zeynali, K.; Maryam Sajjadi, S.; Taherzadeh, F. *Spectrochim. Acta Part A Mol. Biomol. Spectrosc.* **2016**, *153*, 674–680.
(8) López-Palacios, J.; Colina, A.; Heras, A.; Ruiz, V.; Fuente, L. *Anal. Chem.* **2001**, *73*, 2883–2889.
(9) Garoz-Ruiz, J.; Heras, A.; Palmero, S.; Colina, A. *Anal. Chem.* **2015**, *87*, 6233–6239.
(10) Ibañez, D.; Fernandez-Blanco, C.; Heras, A.; Colina, A. *J. Phys. Chem. C* **2014**, *118*, 23426–23433.
(11) Ibañez, D.; Romero, E. C.; Heras, A.; Colina, A. *Electrochim. Acta* **2014**, *129*, 171–176.
(12) Shi, C.; Zhang, W.; Birke, R. L.; Lombardi, J. R. *J. Phys. Chem.* **1990**, *94*, 4766–4769.
(13) Gao, P.; Gosztola, D.; Weaver, M. J. *J. Phys. Chem.* **1988**, *92*, 7122–7130.
(14) Zong, C.; Chen, C. J.; Zhang, M.; Wu, D. Y.; Ren, B. *J. Am. Chem. Soc.* **2015**, *137*, 11768–11774.
(15) Ibañez, D.; Plana, D.; Heras, A.; Fermín, D. J.; Colina, A. *Electrochem. Commun.* **2015**, *54*, 14–17.
(16) Ren, B.; Li, X. Q.; She, C. X.; Wu, D. Y.; Tian, Z. Q. *Electrochim. Acta* **2000**, *46*, 193–205.
(17) Hu, Q.; Hinman, A. S. *Anal. Chem.* **2000**, *72*, 3233–3235.
(18) Kavan, L.; Janda, P.; Krause, M.; Ziegs, F.; Dunsch, L. *Anal. Chem.* **2009**, *81*, 2017–2021.
(19) Gómez, R.; Pérez, J. M.; Solla-Gullón, J.; Montiel, V.; Aldaz, A. *J. Phys. Chem. B* **2004**, *108*, 9943–9949.
(20) Bonifacio, A.; Millo, D.; Gooijer, C.; Boegschoten, R.; Zwan, G. Van Der. *Anal. Chem.* **2004**, *76*, 1529–1531.
(21) Yuan, T.; Le Thi Ngoc, L.; Van Nieuwkasteele, J.; Odijk, M.; Van Den Berg, A.; Permentier, H.; Bischoff, R.; Carlen, E. T. *Anal. Chem.* **2015**, *87*, 2588–2592.
(22) Yu, J.-S.; Yang, C.; Fang, H.-Q. *Anal. Chim. Acta* **2000**, *420*, 45–55.
(23) Gaillard, F.; Levillain, E.; Dhamelincourt, M.-C.; Dhamelincourt, P.; Lelieur, J. P. *J. Raman Spectrosc.* **1997**, *28*, 511–517.
(24) Bellec, V.; De Backer, M. G.; Levillain, E.; Sauvage, F. X.; Sombret, B.; Wartelle, C. *Electrochem. Commun.* **2001**, *3*, 483–488.
(25) Dias, M.; Hudhomme, P.; Levillain, E.; Perrin, L.; Sahin, Y.; Sauvage, F.-X.; Wartelle, C. *Electrochem. Commun.* **2004**, *6*, 325–330.
(26) Güell, A. G.; Meadows, K. E.; Unwin, P. R.; Macpherson, J. V. *Phys. Chem. Chem. Phys.* **2010**, *12*, 10108–10114.
(27) Nützenadel, C.; Züttel, A.; Chartouni, D.; Schlapbach, L. *Electrochem. Solid-State Lett.* **1999**, *2*, 30–32.
(28) Baughman, R. H.; Zakhidov, A. A.; de Heer, W. A. *Science* **2002**, *297*, 787–792.
(29) Katz, E.; Willner, I. *ChemPhysChem* **2004**, *5*, 1084–1104.
(30) Picó, F.; Rojo, J. M.; Sanjuán, M. L.; Ansón, A.; Benito, A. M.; Callejas, M. A.; Maser, W. K.; Martínez, M. T. *J. Electrochem. Soc.* **2004**, *151*, A831–A837.
(31) Ghosh, S.; Sood, A. K.; Kumar, N. *Science* **2003**, *299*, 1042–1044.
(32) Bachtold, A.; Hadley, P.; Nakanishi, T.; Dekker, C. *Science* **2001**, *294*, 1317–1320.
(33) Tans, S. J.; Verschueren, A. R. M.; Dekker, C. *Nature* **1998**, *672*, 669–672.
(34) Star, A.; Tu, E.; Niemann, J.; Gabriel, J.-C. P.; Joiner, C. S.; Valcke, C. *Proc. Natl. Acad. Sci.* **2006**, *103*, 921–926.
(35) Güell, A. G.; Meadows, K. E.; Dudin, P. V; Ebejer, N.; Macpherson, J. V; Unwin, P. R. *Nano Lett.* **2014**, *14*, 220–224.

(36) Garoz-Ruiz, J.; Palmero, S.; Ibañez, D.; Heras, A.; Colina, A. *Electrochem. Commun.* **2012**, *25*, 1–4.
(37) Vilela, D.; Garoz, J.; Colina, Á.; González, M. C.; Escarpa, A. *Anal. Chem.* **2012**, *84*, 10838–10844.
(38) Garoz-Ruiz, J.; Ibañez, D.; Romero, E. C.; Ruiz, V.; Heras, A.; Colina, A. *RSC Adv.* **2016**, *6*, 31431–31439.
(39) Schroll, C. A.; Chatterjee, S.; Heineman, W. R.; Bryan, S. A. *Anal. Chem.* **2011**, *83*, 4214–4219.
(40) Sarkar, C.; Basu, B.; Chakroborty, D.; Dasgupta, P. S.; Basu, S. *Brain. Behav. Immun.* **2010**, *24*, 525–528.
(41) Perez-Costas, E.; Melendez-Ferro, M.; Roberts, R. C. *J. Neurochem.* **2010**, *113*, 287–302.
(42) Lotharius, J.; Brundin, P. *Nat. Rev. Neurosci.* **2002**, *3*, 932–942.
(43) Venton, B. J.; Wightman, R. M. *Anal. Chem.* **2003**, *75*, 414A–421A.
(44) Feng, W.; Li, Y.; Wu, J.; Noda, H.; Fujii, A.; Ozaki, M.; Yoshino, K. *J. Phys. Condens. Matter* **2007**, *19*, 186220.
(45) Lefebvre, M.; Qi, Z.; Rana, D.; Pickup, P. G. *Chem. Mater.* **1999**, *11*, 262–268.
(46) Groenendaal, L.; Zotti, G.; Aubert, P.-H. P. H.; Waybright, S. M.; Reynolds, J. R. *Adv. Mater.* **2003**, *15*, 855–879.
(47) Zanfrognini, B.; Colina, A.; Heras, A.; Zanardi, C.; Seeber, R.; López-Palacios, J. *Polym. Degrad. Stab.* **2011**, *96*, 2112–2119.
(48) Brewster, J. D.; Anderson, J. L. *Anal. Chem.* **1982**, *54*, 2560–2566.
(49) Hawley, M. D.; Tatawawadi, S. V; Piekarski, S.; Adams, R. N. *J. Am. Chem. Soc.* **1967**, *89*, 447–450.
(50) Chen, S.-M.; Peng, K.-T. *J. Electroanal. Chem.* **2003**, *547*, 179–189.
(51) Kavan, L.; Dunsch, L. *ChemPhysChem* **2007**, *8*, 974–998.
(52) Dresselhaus, M. S.; Dresselhaus, G.; Saito, R.; Jorio, A. *Phys. Rep.* **2005**, *409*, 47–99.
(53) Rozlosnik, N. *Anal. Bioanal. Chem.* **2009**, *395*, 637–645.
(54) Hohnholz, D.; Okuzaki, H.; MacDiarmid, A. G. *Adv. Funct. Mater.* **2005**, *15*, 51–56.
(55) Laforgue, A. *J. Power Sources* **2011**, *196*, 559–564.
(56) Liu, R.; Duay, J.; Lee, S. B. *ACS Nano* **2010**, *4*, 4299–4307.
(57) Tintula, K. K.; Sahu, A. K.; Shahid, A.; Pitchumani, S.; Sridhar, P.; Shukla, A. K. *J. Electrochem. Soc.* **2010**, *157*, B1679–B1685.
(58) Vasantha, V. S.; Phani, K. L. N. *J. Electroanal. Chem.* **2002**, *520*, 79–88.
(59) Coletta, C.; Cui, Z.; Archirel, P.; Pernot, P.; Marignier, J.-L.; Remita, S. *J. Phys. Chem. B* **2015**, *119*, 5282–5298.
(60) Fernandez-Blanco, C.; Ibañez, D.; Colina, A.; Ruiz, V.; Heras, A. *Electrochim. Acta* **2014**, *145*, 139–147.

Insert Table of Contents artwork here